MAXIMUM POWER POINT TRACKING OF WIND ENERGY CONVERTION SYSTEM WITH PARMANENT MAGNET SYNCRONOUS GENERATOR

Krishna Kumar Pandey
Student(M.Tech)Power electronics and drives
MMMEC Gorakhpur-273010

Dr.A.N.Tiwari
Associate professor Electrical Dept.
MMMEC Gorakhpur-273010

Abstract

This paper presents a control strategy of a variable speed wind turbine and gets maximum power point tracking which is connected with multipole permanent magnet synchronous generator (PMSM) and fully controlled three phase converter.

The simulation results show that theoretical analysis and the validation of the proposed strategy.

Keywords- Permanent magnet synchronous motor (PMSM), Wind Energy conversion system (WECS), maximum power point tracking (MPPT)

1. Introduction

One of the most commonly used renewable energy; wind power is the most promising for replacing the fossil fuel in the near future. The advancement in power electronics devices has further played an important role in the improvement of their reliability and controllability [2]. The variable-speed wind turbines are more attractive, as they can extract maximum power at different wind velocities, and thus, reduce the mechanical stress on WECS by absorbing the wind-power fluctuations. Recently, PMSG-based directly driven variable-speed WECS are becoming more popular due to the elimination of gear box and excitation system [2][3][4]. Generally shaft-mounted speed sensors are used, resulting in additional cost and complexity of the system. To alleviate the need of these sensors, several speed-estimating algorithms based on motional electromotive force (EMF), flux-linkage variation, However, the precise estimation of rotor position and speed is very difficult as most of these suffer because of simplified computations based on several assumptions, ignorance of parameter variations, and inaccuracy involved with low-voltage signal measurement at lower–speed, especially in case of directly driven PMSG. The wind turbines with full-scale converters will be preferred in future, their are maximum power is the cubic function of generator speed for a given tip speed ratio so for tracking MPPT [1]. We are tacking two close loop which are speed control loop and current control loop [17][19].

2. System description

The system under consideration employs PMSG-based variable speed WECS consisting of three phase full converter and load with a common dc-link. The block diagram of variable speed WECS is shown in Fig.1 and the main components of system with their important characteristics are discussed below:

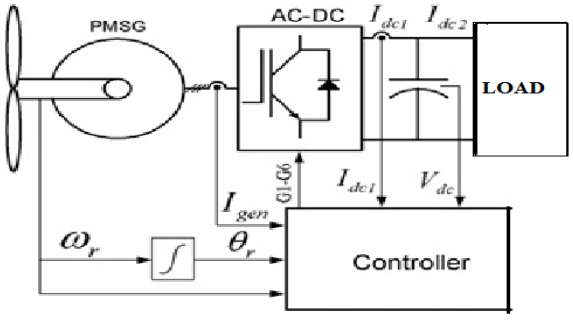

Fig.1 Block diagram of PMSG-based variable speed WECS

2.1 Wind Energy and Wind Turbine

The circulation of air in the atmosphere is caused by the non uniform heating of the earth's surface by sun. In general, during the day the air above the land mass tends to heat up more rapidly than the air over

water. In coastal regions this manifests itself in a strong onshore wind. At night the process is reversed because the air cools down more rapidly over the land and the breeze blows off shore.

2.1.1. Power in wind energy

The power in the wind can be computed by using the concept of kinetics. The wind mill works on the principal of converting kinetic of the wind to mechanical energy [18][20]. We know that power is equal to energy per unit time. The energy available is the kinetic energy of the wind. The kinetic energy of any particle is equal to one half its mass times the square of its velocity, or $\frac{1}{2}mV^2$. The amount of air passing in unit time, through an area A, with velocity V, is A.V, and its mass m is equal to its volume multiplied by its density of ρ air, or

$$m = \rho AV$$

Substituting this value of the mass in the expression for the kinetic energy,

$$kinetic\ energy = \frac{1}{2}\rho AV.V^2$$

$$= \frac{1}{2}\rho AV^3 \text{ watts}$$

Equations tell us that the wind power is proportional to the intercept area. Thus an aero-turbine with large swept area has higher power than a smaller area machine [5][6][7]; Since the area is normally circular of radius r in horizontal axis aero-turbine, then

$$A = \pi r^2$$

So the equation of wind power is converted to

$$Available\ wind\ power\ P_a = \frac{1}{2}\rho\pi r^2 V^3 \text{ watts}$$

Characteristics of wind power depend on the cubic function of wind velocity, which is sown in below.

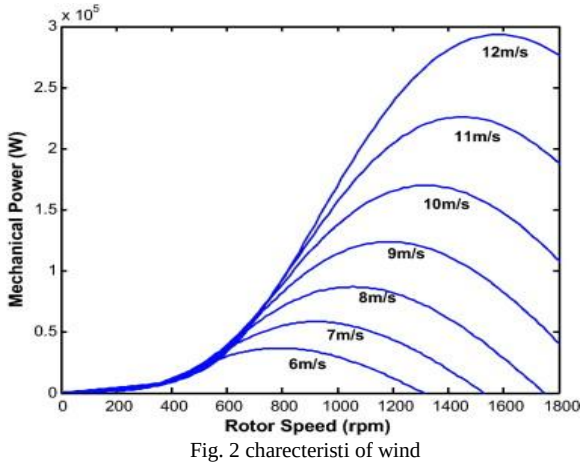

Fig. 2 charecteristi of wind

2.1.2. Wind Turbine

The wind power captured by wind turbine depends on its power co-efficient (Cp) which is given by the relation

$$C_p = \frac{P_{turb}}{P_{Wind}}$$

$$P_{turb} = P_{Wind}C_p = \frac{1}{2}\rho\pi r^2 V^3\ C_p$$

But, for a given turbine C_p is not always constant. The most common parameters for C_p are the tip speed ratio λ and the pitch angle β. The tip speed ratio is given as

$$\lambda = \frac{tip\ speed}{Wind\ speed} = \frac{\omega \cdot r}{V}$$

Here the power coefficient $C_p = \int(\lambda, \beta)$ is a function of both parameters. Consequently, different wind speeds will require the optimal values of tip speed and pitch angle to achieve a high C_p and therefore giving the highest power output at all available wind speeds. The above-mentioned aspects make it very clear that to extract maximum power out of the varying wind we need to have a wind turbine that allows the change in rotor speed to reach optimal aerodynamic conditions [8][9][10].

2.2. Generator

WECS need a low-speed gearless generator, especially for off-shore wind applications, where the geared doubly fed induction generator will require regular maintenance because of tearing wearing in brushes and gear box [5][6]. Both the brushes and the gear box can be eliminated from WECS by using directly coupled low speed generators. Further, the elimination of the gear box can increase the efficiency of wind turbine by 10%.

The low-speed PMSG requires:

1. Higher number of poles to obtain suitable frequency at low speed;
2. Big rotor diameter for the high wind turbine torque

2.2.1. E.M.F. Equation of an alternator

The expression for induced emf and torque is' derived for a machine with P poles, Z_p coil sides in series per phase in a field with a flux per pole of Φ , T turns per phase, *f* frequency and rotating at n rps(N rpm). Since the flux per pole is Φ, each stator

conductor cuts a flux P Φ. The average value of generated voltage per conductor

$$= \frac{\text{flux cut per revolution in Wb}}{\text{Time taken for one revolution in seconds}}$$

The average voltage generated per conductor

$$E_{av}/Conductor = \frac{\text{P}\,\Phi}{1/_n} = n\text{P}\,\Phi \quad \text{volts} \qquad \text{..... (1)}$$

We know that

$$f = \frac{\text{PN}}{120} = \frac{Pn}{2}$$

$$Pn = 2f$$

Substituting the value of *Pn* in eq (1),we get

$$E_{av}/Conductor = 2f\,\Phi$$

Since there are Z_p conductors in series per phase, the average voltage generated per phase is given by

$$E_{av}/phase = 2f\,\Phi Z_p$$

Since one turn or coil has two sides, $Z_p=2T_p$, and the expression for the average generated voltage per phase can be written as

$$E_{av}/phase = 4f\,\Phi T_p$$

For the voltage wave, the form factor is given by

$$k_f = \frac{r.m.s.value}{average\ value}$$

For a sinusoidal voltage, $k_f=1.11$. Therefore, the r.m.s. value of the generated voltage per phase can be written as

$$E_{r.m.s.}/phase = k_f \times E_{av}/phase = 1.11 \times 4f\,\Phi T_p$$

$$E_p = 4.44f\Phi T_p$$

For rotating machine the winding factor (K_w) is involved in E.M.F. equation which is denoted by

$$E_p = 4.44K_w f\Phi T_p$$

$$E_p = 4.44K_c K_d f\Phi T_p$$

Where $K_w = K_c K_d$

For full pitch coil, $K_c=1$;

For concentrated winding, $K_d=1$;

2.2.2. Equivalent Circuit And Modelling of PMSG:

Since the back-EMF is the function of rotor position in stationary reference frame, therefore, it is convenient to model PMSG in this frame. The voltage equations of PMSG are as follows

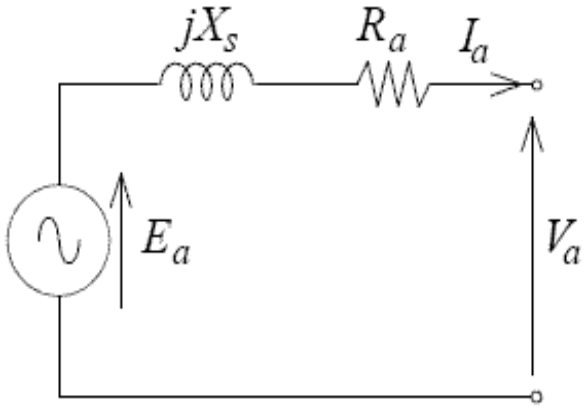

Fig. 3equvalent circuit diagram of PMSM

$$V_\alpha = -R_a i_\alpha - X_s \frac{di_\alpha}{dt} + E_\alpha$$

$$V_\beta = -R_a i_\beta - X_s \frac{di_\beta}{dt} + E_\beta$$

where V_α ,V_β are stator terminal voltages, R_a is stator resistance, X_S is stator inductance, i_α, i_β are output currents, and E_α, E_β are back EMFs, which can be given as

$$E_{\alpha,\beta} = \begin{bmatrix} E_a \\ E_\beta \end{bmatrix} = \omega_r \lambda_m \begin{bmatrix} -\sin(\theta_r) \\ \cos(\theta_r) \end{bmatrix}$$

Here, ω_r , θ_r , and λ_m are rotor speed, rotor position, and magnetic-flux linkage, respectively

On rearranging (1) and (2), and rewriting them in matrix form, we have

$$\begin{bmatrix} \dot{i}_\alpha \\ \dot{i}_\beta \end{bmatrix} = \begin{bmatrix} -R_a/X_s & 0 \\ 0 & -R_a/X_s \end{bmatrix} \begin{bmatrix} i_\alpha \\ i_\beta \end{bmatrix}$$

$$+ \begin{bmatrix} -1/X_s & 0 \\ 0 & -1/X_s \end{bmatrix} \left(\begin{bmatrix} V_\alpha \\ V_\beta \end{bmatrix} - \begin{bmatrix} E_\alpha \\ E_\beta \end{bmatrix} \right)$$

Hear the transfer function modelling is arrange in a equation

$$\dot{i}_{\alpha,\beta} = A \cdot i_{\alpha,\beta} + B \cdot \left(V_{\alpha,\beta} - E_{\alpha,\beta} \right)$$

where the dot '·' indicates the estimated variables and

$$A = \begin{bmatrix} -R_a/X_s & 0 \\ 0 & -R_a/X_s \end{bmatrix}$$

$$B = \begin{bmatrix} -1/X_s & 0 \\ 0 & -1/X_s \end{bmatrix}$$

,

$$i_{\alpha,\beta} = \begin{bmatrix} i_\alpha \\ i_\beta \end{bmatrix} \qquad i_{\alpha,\beta} = \begin{bmatrix} i_\alpha \\ i_\beta \end{bmatrix}$$

$$V_{\alpha,\beta} = \begin{bmatrix} V_\alpha \\ V_\beta \end{bmatrix} \qquad E_{\alpha,\beta} = \begin{bmatrix} E_\alpha \\ E_\beta \end{bmatrix}$$

, and

The state-space-equivalent diagram of equation is shown in below

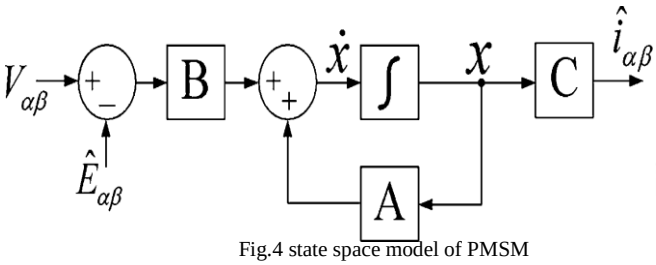

Fig.4 state space model of PMSM

2.3. Power electronics interference

The proposed system consists of fully controlled converters decoupled by a dc-link [21][22]. The converters have been realised by using six switches for converter. The thyristors require small reactors in series to limit the rate of rise of currents and snubbers[11][12], Which are resistors in series with capacitors across the devices are commutated.

2.3.1 Mathematical modelling and circuit diagram

If the line-to-neutral voltages are defined as

$$v_{an} = V_m \sin \omega t$$

$$v_{bn} = V_m \sin(\omega t - \frac{2\pi}{3})$$

$$v_{cn} = V_m \sin(\omega t + \frac{2\pi}{3})$$

The corresponding line-to-line voltage are,

$$v_{ab} = v_{an} - v_{bn} = \sqrt{3} V_m \sin(\omega t + \frac{\pi}{6})$$

$$v_{bc} = v_{bn} - v_{cn} = \sqrt{3} V_m \sin(\omega t - \frac{\pi}{2})$$

$$v_{ca} = v_{cn} - v_{an} = \sqrt{3} V_m \sin(\omega t + \frac{\pi}{2})$$

The average output voltage is found from

$$V_{dc} = \frac{3}{\pi}\int_{\pi/6+\alpha}^{\pi/2+\alpha} v_{ab}\, d(\omega t) = \frac{3}{\pi}\int_{\pi/6+\alpha}^{\pi/2+\alpha} \sqrt{3}\, V_m \sin\left(\omega t + \frac{\pi}{6}\right) d(\omega t)$$

$$= \frac{3\sqrt{3}V_m}{\pi}\cos\alpha$$

A typical inversion mode of operation is shown in Figure 2.8. Note that this corresponds to a second-quadrant operation of the dc motor drive.

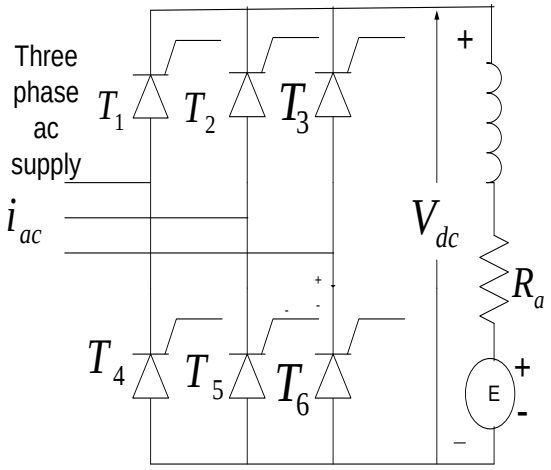

Fig.5 Three phase controlled converter

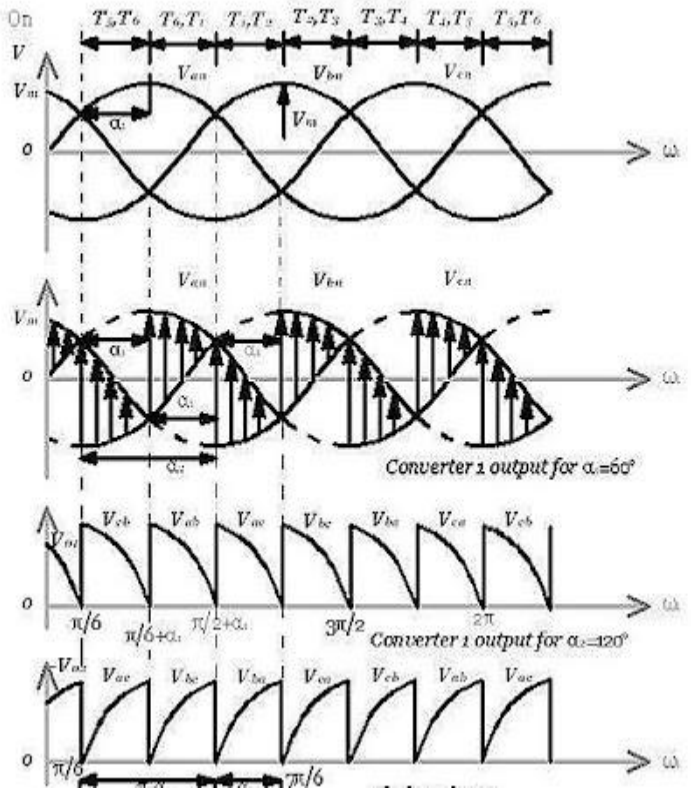

Fig. 6 wave form of controlled rectifier

The maximum average output voltage for delay angle $\alpha = 0$, is

$$V_{dm} = \frac{3\sqrt{3}V_m}{\pi}$$

And the normalized average output voltage is

$$V_n = \frac{V_{dc}}{V_{dm}} = \cos\alpha$$

The rms value of the output voltage is found from

$$V_{rms} = \left[\frac{3}{\pi}\int_{\pi/2+\alpha}^{\pi/2+\alpha} 3\left(V_m \sin\left(\omega t + \frac{\pi}{6}\right)\right)^2 d(\omega t)\right]^{1/2}$$

$$= \sqrt{3}V_m\left(\frac{1}{2} + \frac{3\sqrt{3}}{4\pi}\cos 2\alpha\right)^{1/2}$$

3. Development of proposed control strategy

In a variable speed WECS, the maximum power at different wind velocities is almost a cubic function of generator speed as shown in Fig.7. Therefore the generator speed is controlled in order to follow the power-speed characteristic. For this purpose, the power at dc-link is used to obtain reference speed by using the power-speed curve of the generator [14][15]. The error of this reference speed and actual speed are then given to the proportional-integral (PI) regulator to obtain reference torque of the generator expressed as

$$T_g^* = \left(K_{P\omega} + \frac{K_{I\omega}}{S}\right)(\omega_r^* - \omega_r)$$

Where $K_{P\omega}$, $K_{I\omega}$ are proportional and integral gains for generator speed control. The q-axis reference current component (torque controlling current component) can be derived using

$$i_q^* = \frac{4}{3}\left(\frac{T_g^*}{P\lambda_m}\right)$$

The d-axis reference current component can be set to zero in order to obtain maximum torque at minimum current and therefore to minimise the resistive losses in the generator [16] . The generator-side control diagram is shown in Fig. 7.

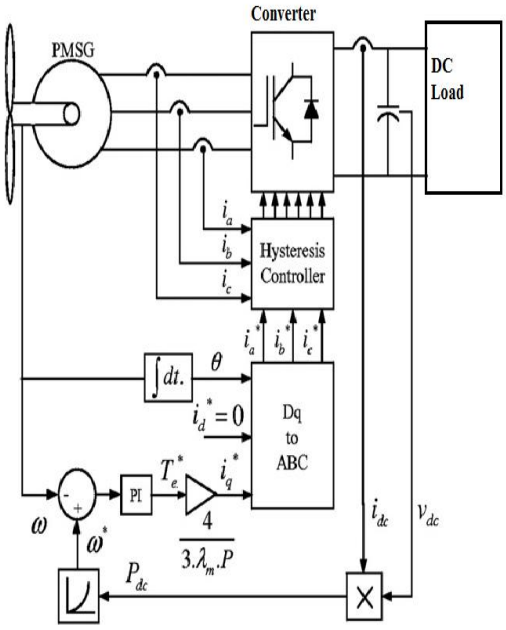

fig.7 Proposed model

4. Simulation and results

The proposed control strategy for PMSG-based variable speed WECS is simulated on MATLAB/SIM POWER SYSTEM in different operating conditions. The simulink model shows that, the stator current fluctuation in nearly proportional to fluctuation occurred in wind speed, due to the closed loop scheme. Three phase stator current converted into dc through the three phase fully controlled rectifier as shown in figure 9. The DC output power as shown in fig 11 and fig 12 converted in to wind speed in equivalent of wind power then by comparing with the generator speed and given error signal to the 2 phase to 3 phase converter as shown in fig.13. Then the output passed through the hysteresis controller to obtain the pulses in convertor as shown in fig.14.

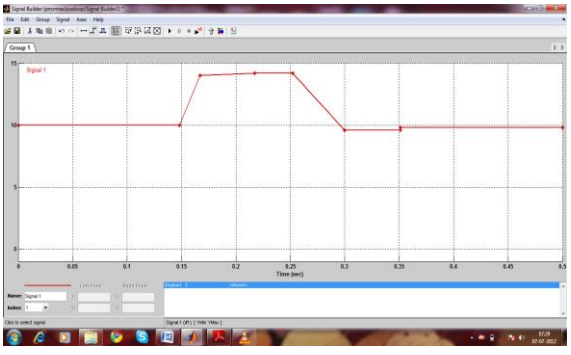

Fig. 8 wind speed

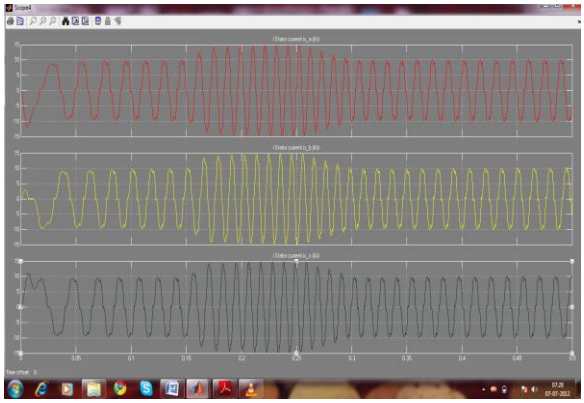

Fig.9 Three phase current of generator

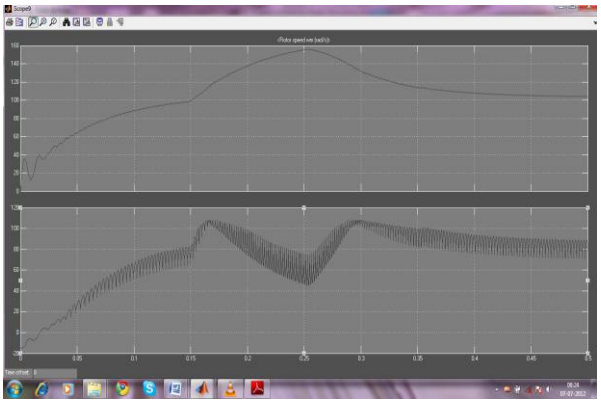

Fig. 13 speed Comparator

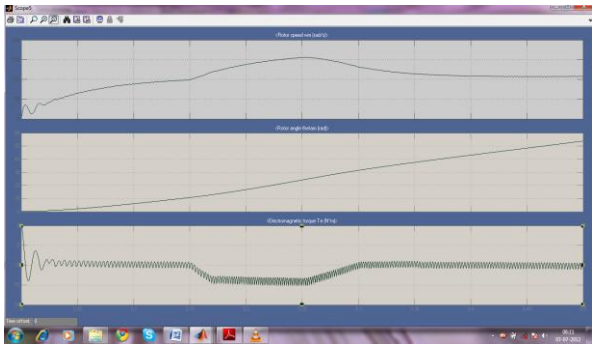

Fig.10 Rotor speed, angle & torque

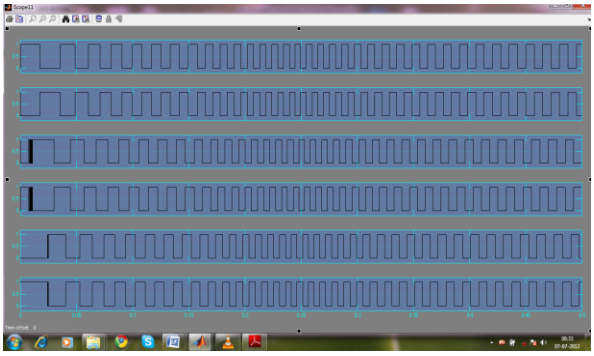

Fig. 14 Pulses for the controlled rectifier

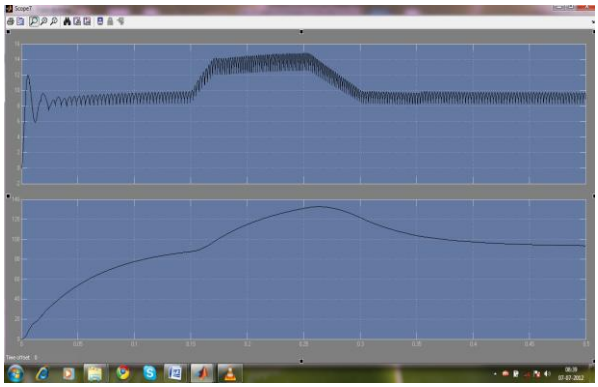

Fig.11 DC output current and voltage

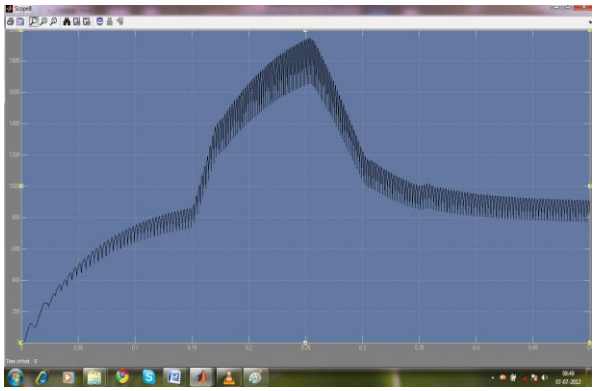

Fig.12 DC power

5. Conclusions 1

This paper shows that the maximum power is traced on implementing closed loop scheme to remove fluctuation occurred in the output by maintaining the switching in the form of pulses on application of controlled rectifier.

6. References

[1] MORREN J and DE HANN S.W : ‘‘Ride-through of wind turbines with doubly-fed induction generator during a voltage dip’’, IEEE Trans. Energy Convers., 2005 , 20 , (2) , pp. 435–441

[2] ‘‘Connection of wind turbines at the grid under100 kV’’, Technical regulations T.F. 3.2.6, Eltra/Elkraft,July2004.Internet, http://www.eltra.dk

[3] SENJYU T., KINJO T. and FUJITA H., AICHI : ‘‘Analysis of terminal voltage and output power control of wind turbine generator by series and parallel compensation using SMES’’, IEEE 35th Ann. Power Electronics Specialists Conf., June 2004, vol. 6, pp. 4278–4284.

[4] SACCOMANDO G., SVENSSON J., SANNINO A : ‘‘Improving voltage disturbance rejection for variable-speed wind turbines’’, IEEE Trans. Energy Convers., 2002, 17, (3), pp. 422–428

[5] MILLIGAN M : ‘‘Measuring wind plant capacity value’’, (National Renewable Energy Laboratory, Golden Colorado, USA)

[6] T. Senjyua, S. Tamakia, E. Muhandoa, N. Urasakia, H. Kinjoa, T. Funabashib, H. Fujitac, and H. Sekinea, ‘‘Wind velocity and rotor position sensorless maximum power point tracking control for wind generation system’’, in Proc. 30th Annu. Conf. IEEE Ind. Electron. Soc. (IECON 2004), vol. 2, pp. 1957–1962.

[7] S. Bhowmik and R. Sp´ee, ‘‘Wind speed estimation based variable speed wind power generation’’, in Conf. Rec. IEEE IECON 1998, Aachen, Germany, pp. 596–601.

[8] ‘‘Capacity factors at Kansas wind farms compared with total state electrical demand’’, July 2007 to June 2008, http://www.kcc.state.ks.us/energy/charts/Wind Capacity Factors at Kansas Wind Farms Compared with Total State Electrical Demand.pdf

[9] BOCCARD N : ‘‘Capacity factor of wind power realized values vs. estimates’’, Elsevier Trans. Energy Policy, 2009, 37, pp. 2679–2688

[10] G. Saccomando, J. Svensson, and A. Sannino, ‘‘Improving voltage disturbance rejection for variable-speed wind turbines’’, *IEEE Trans. Energy Convers.*, vol. 17, no. 3, pp. 422–428, Sep. 2002

[11] MULJADI E. and BUTTERFIELD C.P : ‘‘Pitch-controlled variable speed wind turbine generation’’, IEEE Trans. Ind. Appl., 2001, 37, (1), pp. 240–246

[12] J.Morren, S.W. de Hann, ‘‘Ride-through of wind Turbines with doublyfed induction generator during a voltage dip’’, IEEE Trans. Energy Convers., vol. 20, no. 2, pp. 435–441, Jun. 2005

[13] HEIER S : ‘‘Grid integration of wind energy conversion systems’’ (Wiley, Chicester, UK, 1998)

[14] B. K. Bose, ‘‘Modern Power Electronics and AC Drives’’, Upper Saddle River, NJ: Prentice-Hall, 2002.

[15] JOHNSON G : ‘‘Wind energy systems’’ (Prentice-Hall, Englewood Cliffs, NJ, 1990)

[16] ASIMINOAEI L., BLAABJERG F. and HANSEN S : ‘‘Harmonic detection methods for active power filter applications’’, IEEE Ind. Appl. Mag., 2007, pp. 22–33

[17] WESTLAKE A.J.G., BUMBY J.R. and SPOONER E : ‘‘Damping the powerangle oscillations of a permanent magnet synchronous generator with particular reference to wind turbine applications’’, IEE Proc. Electr. Power Appl., 1996, 143, (3)

[18] LEONHARD W : ‘‘Control of electric drives’’ (Springer, New York, 1997)

[19] KRAUSE P.C., WASYNCZUK O. and SUDHOFF S.D : ‘‘Analysis of electric machinery’’ (IEEE Press, 1994)

[20] SLOOTWEG J.G., DE HAAN S.W.H., POLINDER H. and KLING W.L : ‘‘General model for representing variable speed wind turbines in power system dynamics simulations’’, IEEE Trans. Power Syst., 2003, 18, (1), pp. 144–151

[21] CARRASCO J.M., FRANQUELO L.G., BIALASIEWICZ J.T. and ET AL : ‘‘Power-electronic systems for the grid integration of renewable energy sources: a survey’’, IEEE Trans. Ind. Electron., 2006, 53, (4), pp. 1002–1016

[22] ENSLIN J.H.R. and HESKES P.J.M : ‘‘Harmonic interaction between a large number of distributed power inverters and the distribution network’’, IEEE Trans. Power Electron., 2004, 19, (6), pp. 1586–1593